



HAL
open science

Quantum transport properties of gas molecules adsorbed on Fe doped armchair graphene nanoribbons: A first principle study

Hachemi Zitoune, Christophe Adessi, Lotfi Benchallal, Madani Samah

► To cite this version:

Hachemi Zitoune, Christophe Adessi, Lotfi Benchallal, Madani Samah. Quantum transport properties of gas molecules adsorbed on Fe doped armchair graphene nanoribbons: A first principle study. *Journal of Physics and Chemistry of Solids*, 2021, 153, pp.109996. 10.1016/j.jpcs.2021.109996 . hal-03175972

HAL Id: hal-03175972

<https://hal.science/hal-03175972>

Submitted on 15 Mar 2023

HAL is a multi-disciplinary open access archive for the deposit and dissemination of scientific research documents, whether they are published or not. The documents may come from teaching and research institutions in France or abroad, or from public or private research centers.

L'archive ouverte pluridisciplinaire **HAL**, est destinée au dépôt et à la diffusion de documents scientifiques de niveau recherche, publiés ou non, émanant des établissements d'enseignement et de recherche français ou étrangers, des laboratoires publics ou privés.



Distributed under a Creative Commons Attribution - NonCommercial 4.0 International License

Quantum transport properties of gas molecules adsorbed on Fe doped armchair graphene nanoribbons: A first principle study

Hachemi Zitoune^{a,b,d}, Christophe Adessi^b, Lotfi Benchallal^c, Madani Samah^d

^aLaboratoire LM2D, Equipe PhyMo, Université Akli Mohand Oulhadj, Bouira, Algérie

^bUniv Lyon, Université Claude Bernard Lyon 1, CNRS, Institut Lumière Matière, F-69622, Villeurbanne, France

^cUniversité Houari Boumediène, Laboratoire Physique des Matériaux, USTHB, Alger, Algérie

^dUniversité A/Mira, Bejaia, Algérie

Abstract

Graphene, when doped with transition metals, is considered, both experimentally and theoretically, as a good candidate for the detection of gas molecules as CO, CO₂, NO or NO₂. This opens new perspectives for gas sensor set-ups considering that devices based on 2 dimensional graphene are more sensitive to detect molecules than solid-state gas sensors. The state of the arts on gas adsorption on Fe doped armchair graphene nanoribbons (Fe-AGNR) is still in its starting phase and thorough investigations of the mechanism of the adsorption on graphene need to be done. In the present work, the electronic and transport properties of molecules adsorbed on Fe-AGNR are scrutinized using *ab-initio* calculations. We observe that the adsorption of gas molecules on Fe-AGNR changes significantly the electronic properties of both the valence and the conduction band. Besides, The adsorbed molecules change the local electron density of states of the graphene nanoribbons, modifying thus the conductivity, being one of the main output quantity of the gas sensors. We also observe that the adsorbed molecules induce specific impurity bands which play a role in the transport properties. Finally, considering the observed variations of electrical conductance induced by the molecules, we propose several strategies to set-up gas sensors for CO, CO₂, NO and NO₂ molecules. These strategies are either based on the measurement of the conductance in the valence or the conduction band (using either p or n-doped Fe-AGNR) or to the spin polarization induced by the NO and NO₂ molecules.

Keywords: Fe doped graphene nanoribbons, gas adsorption, gas sensor, *ab initio*, DFT, electronic transport

1. Introduction

Due to its mechanical, structural and electronic properties, graphene has a significant potential in the most advanced technological applications [1–5]. It has been subjected to a great upsurge in research since its discovery by Novoselov *et al.* [6]. Indeed, graphene has a very high electron mobility [7, 8] and a great stability on the nanometric scale [9]. It can be produced over large areas and these appealing properties open the perspective to manufacture electronic devices, such as graphene based gas sensors [10–15] which could be more sensitive than conventional devices.

For this kind of 2 dimensional materials, tiny structural modifications have significant effects on their electronic properties. Indeed, graphene nanoribbons with

armchair edges are predicted to be either metallic or semiconducting depending on their dimensions [16, 17]. Furthermore, the electronic properties are very sensitive to the geometry of the edges [18], and the band-gap of graphene nanoribbons can be engineered by means of edge corrugations [19]. For instance, edge disordering is likely to induce a localization regime [20] or to induce resonances [21], edge decorations [22] are likely to modify the transport properties and transition metal decorations is responsible of the formation of transport gap [23]. Structural defects [24] and chemical doping [25, 26] have a major influence on the properties of graphene and graphene nanoribbons as well. For instance, conductance quantization is observed in strongly disordered graphene [27] and it is observed that the location of the dopants on the graphene nanoribbons affects the transport properties [28, 29]. Notably, substitution doping by transition metals is found to be stable and energetically more favorable for gas adsorption [30–32].

Email address: christophe.adessi@univ-lyon1.fr
(Christophe Adessi)

Among the transition metals, Fe has attracted great attention due to the ability to perform Fe substitutional doping by electron beam irradiation [33]. Indeed, Beriyorov *et al.* [34] have shown that the transport properties of Fe doped graphene nanoribbons are more sensitive to CO₂ adsorption with Fe in substitution rather than adsorption. Moreover, it has been shown that Fe doped graphene exhibits high sensitivity to NO [35] molecules for instance. This definitely makes Fe doped graphene a very good candidate for gas detection compared to other 2 dimensional materials as hexagonal transition metal dichalcogenide [36] or hexagonal boron nitride [37]. Concerning the magnetic properties, it has been shown that graphene with substitutional Fe impurity has no magnetic property [26]. However, depending on the number of Fe atoms, armchair graphene nanoribbons (AGNR) can either have non magnetic or magnetic properties [38].

In this work, we have focused on the effects of the adsorption of toxic gas molecules on the electrical and transport properties using density functional theory (DFT) and Green's function formalism. We have considered a semiconducting Fe doped AGNR (decorated at its edges with hydrogen) since the main effects of molecule adsorption on the transport are observed in the valence and the conduction bands. We have considered here 4 of the most common molecules: CO, CO₂, NO and NO₂. The aim of this work is to pinpoint the effects of these molecules on the electrical conductance in order to propose strategies to design graphene-based gas sensors using electron or hole doping.

2. Theory & atomic structure

The results presented here are based on first principle DFT calculations performed with the *ab initio* package SIESTA [39]. All the calculations are done within the generalized gradient approximation parametrized by Perdew, Burke and Ernzerhof [40]. We have used the norm-conserving non relativistic pseudopotential proposed by Trouillier Martin [41] and a double-zeta-polarized basis for all the species.

The energy cut-off of the real-space grid used for the electronic density (and so forth for the Hartree and exchange-correlation potentials) is 400 Ry combined with a Monkhorst-pack grid of $1 \times 16 \times 1$ k-points. The atomic structures have been relaxed with a threshold of 10^{-2} eV/Å for the forces. The unit cells correspond to AGNR composed of 120 atoms passivated on their edges by hydrogen atoms and doped by substituting a carbon with an iron atom (the doped system is denoted hereafter Fe-AGNR) with or without gas molecules

on top of it. The unit cell dimensions are $a = 35$ Å $b = 17.27$ Å and $c = 25$ Å. The a and c directions correspond to vacuum and the c vector is perpendicular to the AGNR.

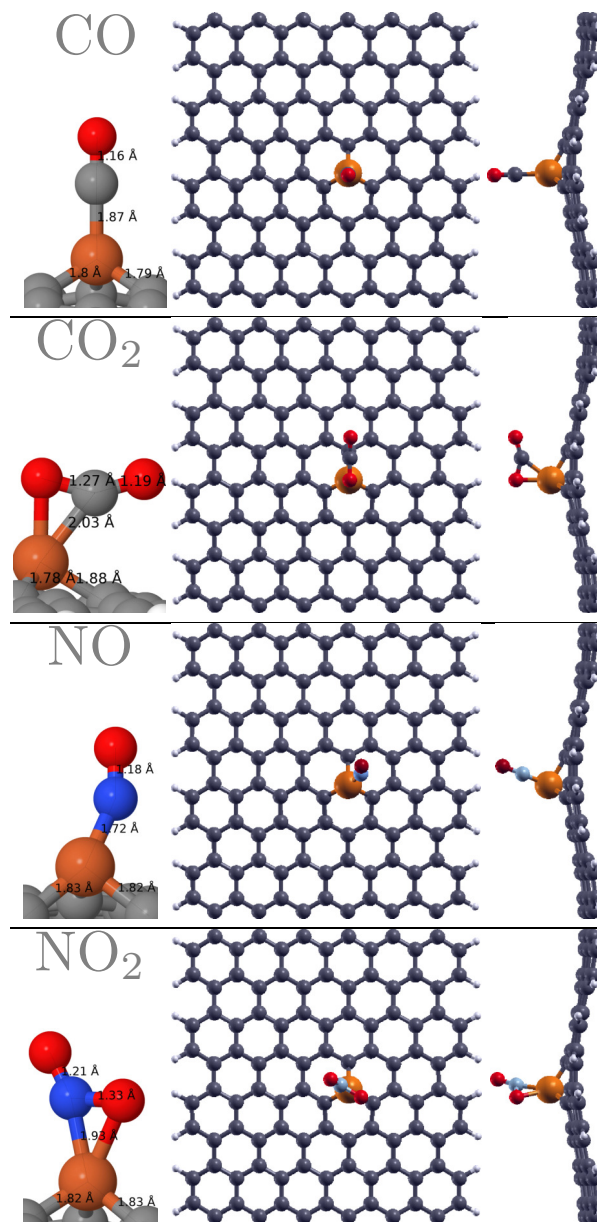


Figure 1: Molecular representation of the Fe-AGNR (Fe doped Armchair Graphene Nanoribbons) unit cells with the adsorbed molecules (from top to bottom CO, CO₂, NO and NO₂) on top of the Fe atom (in substitution of a carbon). On the left are given the typical bond lengths.

The structures of Fe-AGNR with the adsorbed molecules are presented in Fig. 1. Two dimensional

graphene nanoribbons, exhibit slight corrugations when a carbon atom is substituted with an iron one. These deformations of the graphene plane may be attributed to the large atomic radius of iron which protrudes from the plane and thus corrugates its surface on a large distance. The gas molecules when adsorbed on the Fe atom do not affect this corrugation and the atomic structure remains almost the same. The distance between the Fe atom and the nearest carbon atoms is around 1.80 Å and the distance between the Fe atom and the graphene median plane is 1.68 Å. **The binding energy¹ of Fe-AGNR is 7.45 eV which is in good agreement with the 7.14 eV found in Ref. 35.**

The adsorption energies² for CO, CO₂, NO and NO₂ are -2.4 eV, -1.3 eV, -3.1 eV and -3.0 eV respectively. When compared to the direct adsorption on graphene (without iron), it is found that it is more stable when the molecules are adsorbed on top of the Fe atom. Indeed, in Ref. 42 they found for the direct adsorption of CO an energy of -1.34 eV, for CO₂ an energy of -0.31 eV, for NO an energy of -2.29 eV and for NO₂ an energy of -2.70 eV. A similar observation has been done for formaldehyde onto Fe-doped graphene [43]. These observations are a good omen as the main motivation to consider Fe-AGNR for toxic gas detection is linked with the fact that the variations of the electronic and transport properties are enhanced when the molecules are adsorbed on top of the Fe atom when compared to direct adsorption [34, 44–46].

The transport properties are obtained using the Landauer formalism combined with the *ab initio* calculations. In the linear response regime, the electrical conductance can be written as:

$$G = -\frac{2e^2}{\hbar} \int_{-\infty}^{+\infty} T(E) \left(\frac{\partial f}{\partial E} \right) dE, \quad (1)$$

where e the magnitude of the electron charge, \hbar the Planck's constant, f the Fermi distribution and $T(E)$ the energy dependent transmission. In this expression

¹The binding energy is defined as: $E_b = E_{\text{Fe-AGNR}} - (E_{\text{v-AGNR}} + E_{\text{Fe}})$, where $E_{\text{Fe-AGNR}}$, $E_{\text{v-AGNR}}$ and E_{Fe} are respectively the total energy of Fe-AGNR, defective AGNR with a vacancy and Fe atom.

²For instance, the adsorption energy for CO is defined as: $E_{\text{ad}} = E_{\text{CO-Fe-AGNR}} - (E_{\text{Fe-AGNR}} + E_{\text{CO}})$, where $E_{\text{CO-Fe-AGNR}}$, $E_{\text{Fe-AGNR}}$ and E_{CO} are respectively the total energy of Fe-AGNR with CO adsorbed on top of Fe, Fe-AGNR and an isolated CO molecule. The same formulation applies for the other molecules.

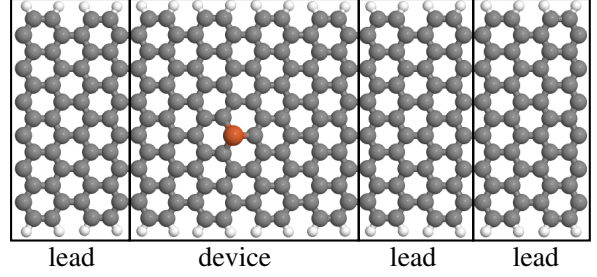


Figure 2: **Molecular representation of the Fe-AGNR unit cell used for the transport calculations. The block denoted “device” contains the defect and the blocks denoted “lead” correspond to pristine AGNR.**

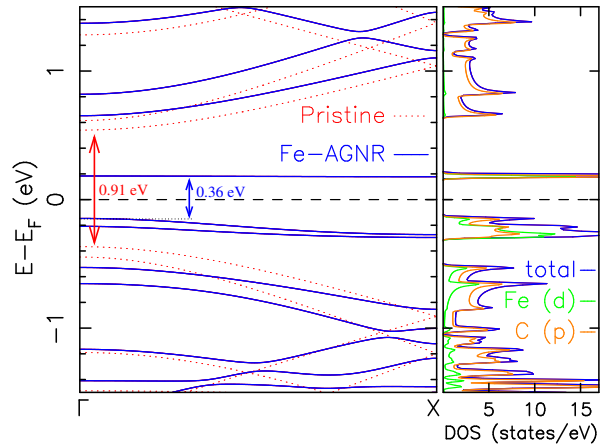


Figure 3: Left figure: Band structure for pristine AGNR (red dotted lines) and Fe-AGNR (blue lines). Right figure: Total and projected density of states (PDOS) for Fe-AGNR. The PDOS is given for the d orbitals of the Fe atom and for the p orbitals of the carbon atoms. The X point corresponds to $k_y = \pi/b$.

the constant $\frac{2e^2}{\hbar}$ is the conductance quantum denoted G_0 hereafter.

The transmission is derived from the Fisher-Lee relation [47]:

$$T(E) = \text{Tr} [\Gamma_L G^r \Gamma_R G^a], \quad (2)$$

where $G^{r(a)}$ is the retarded (advanced) Green's function and $\Gamma_{L(R)}$ the coupling between the left (right) lead and the device. In this work, we consider for the leads pristine AGNR with 60 atoms and for the section of the device which contains the defects 120 atoms plus the adsorbed molecule. **The Hamiltonian matrices used to compute the Green's functions are extracted from a SIESTA calculation with a cell containing 300 atoms (plus the molecule). The cell and its cutout is depicted in Fig. 2. For consistency reasons, all the Hamiltonian matrices are extracted from this single SIESTA calculation. The 2 blocks denoted “lead” at the far right are**

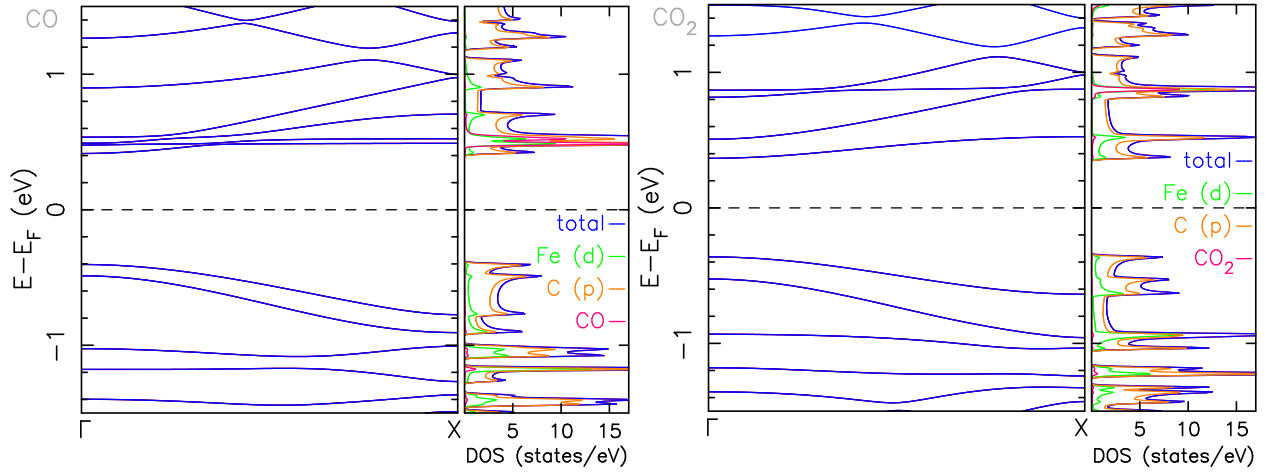


Figure 4: band structure along with DOS and the PDOS for Fe-AGNR with either a CO (left figure) or a CO₂ (right figure) molecule adsorbed on top of the Fe atom. The PDOS corresponds to the projection on the d orbitals of the Fe atom, the projection on the p orbitals of the C atoms and the projection on the orbitals of the CO or CO₂ molecule. The X point corresponds to $k_y = \pi/b$.

used to build the left and right surface Green's functions of the leads. The block denoted "lead" at the far left is used to obtain the hamiltonian matrix linking the left lead and the device. More details on the Green's functions formalism and the technique used here can be found in Ref. 48. It is equivalent to the formalism presented in Ref. 49 for instance.

3. Electronic properties

In Fig. 3 is given the band structure, the density of states (DOS) and the projected density of states (PDOS) of pristine AGNR and Fe-AGNR. The PDOS is given for the predominant orbitals *i.e.* the d orbitals of the Fe atom and the p orbitals of the carbon ones. For Fe-AGNR, we do not observe any spin polarization conversely to other dopants as Ag [30] or Au [50]. The arm-chair graphene nanoribbon considered here has a semi-conducting behavior with a gap about 0.91 eV. When a carbon atom is substituted with a Fe one, the bandgap drops to 0.36 eV. However, this variation of the gap is linked with the occurrence of 3 bands with low dispersion just below and above the Fermi level. These bands can be considered as impurity bands *i.e.* bands induced by the impurity given that the PDOS of the d orbitals of Fe clearly exhibit a predominant weight. This suggests a localization of the corresponding eigenstates. It should be note that these bands are not involve in the transport and do not lead to conduction channels when we consider an isolated Fe atom within the Landauer formalism.

For Fe-AGNR, the bands above the impurity bands in the conduction band (CB) are only due to the carbon atoms as the weight of the orbitals of Fe in the DOS is negligible. These bands are equivalent to the native bands of AGNR. The same behavior is observed for the bands below -0.4 eV in the valence band (VB) which are almost equivalent to those observed for pristine AGNR with, however, a significant weight of the PDOS of the Fe atom in the DOS. This is linked with a large hybridization between the Fe atom and the neighbor carbons with a strong bonding involving the 3d and 4s orbitals of Fe and the 2s and 2p orbitals of the carbons [38, 51].

Fig. 4 depicts the band structures, the DOS and PDOS of Fe-AGNR with either CO or CO₂ adsorbed on top of the Fe atom. For CO, we observe almost undispersed bands at the bottom of the CB. For these bands, the most significant weight in the DOS comes from the CO molecule with also an important contribution from the d orbitals of the Fe atom. They do actually correspond to the 3 impurity bands observed for Fe-AGNR in Fig. 3 which are shifted at higher energy in the the CB when the CO molecule is adsorbed. For CO₂ we also observe a band with a significant weight of the PDOS of the Fe atom at the bottom of the CB. Conversely to the case of CO, this band does not involve the orbitals of the CO₂ molecule. The impurity band involving the molecule is observed at higher energy in the CB. The top of the VB is almost unaffected by the molecules and there is no impurity band. Surprisingly, the weight of the PDOS of the Fe

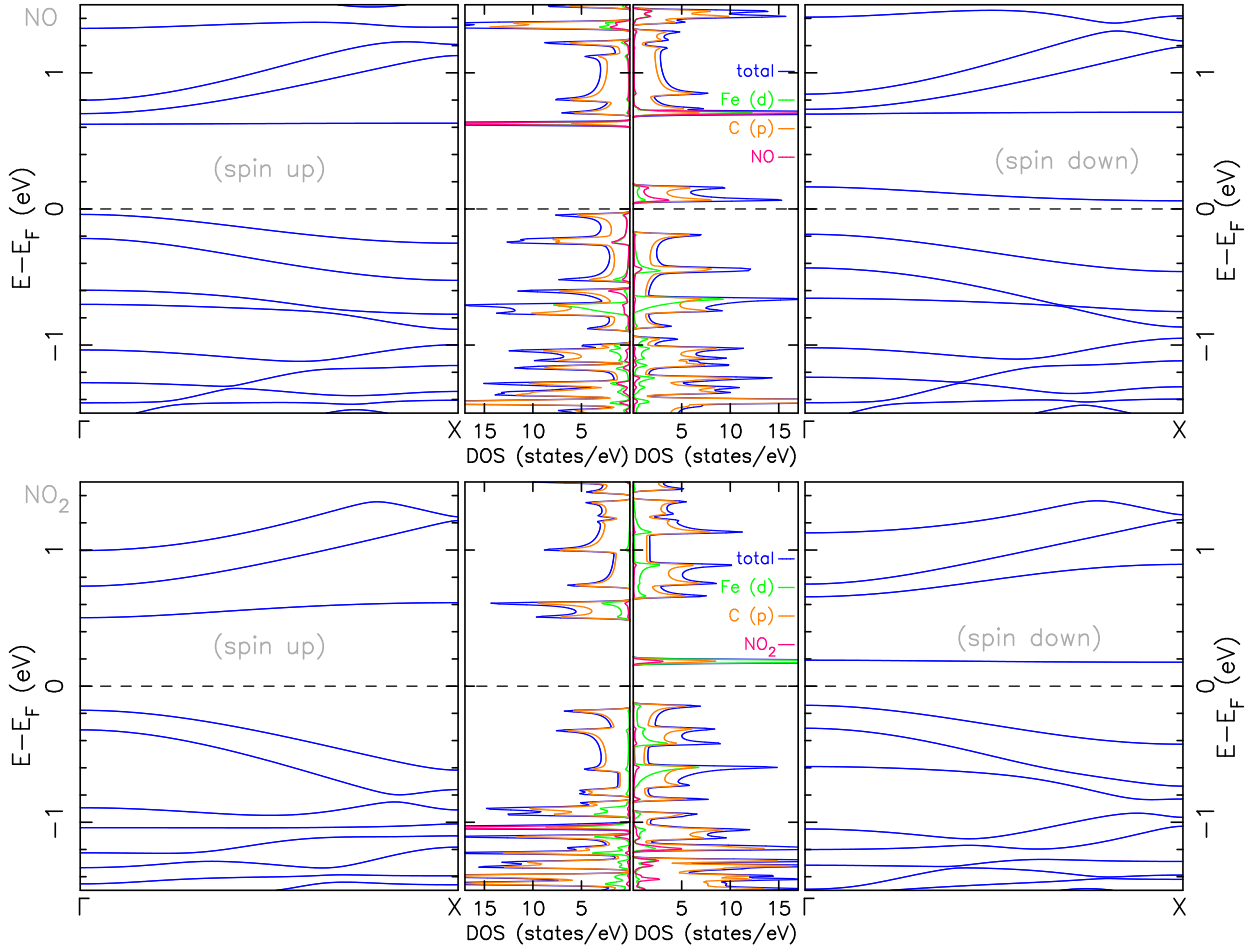


Figure 5: band structure along with the DOS and the PDOS for Fe-AGNR with either a NO (top figures) or a NO₂ (bottom figures) molecule adsorbed on top of the Fe atom. The systems are spin-polarized and thus both spins are represented. The PDOS corresponds to the projection on the d orbitals of the Fe atom, the projection on the p orbitals of the C atoms and the projection on the orbitals of the NO or NO₂ molecule. The X point corresponds to $k_y = \pi/b$.

atom in the DOS is a little bit less important when compare to the case of Fe-AGNR.

For NO and NO₂ molecules, we do observe a spin polarization of the systems. **This is a direct consequence of the paramagnetic property of these molecules (conversely to CO and CO₂ which are diamagnetic) and it is linked with the even number of electrons of nitrogen. The total magnetic moment is $1\mu_B$ and is substantially localized around the NO and NO₂ molecules. For instance, with the NO molecule, the decomposition of the magnetic moment is $1\mu_B$ for the N atom, $0.2\mu_B$ for the O atom and $-0.8\mu_B$ for the Fe atom. The remaining moments are due to the surrounding C atoms.** The band structures, the DOS and the PDOS depicted in Fig. 5 are thus given for both spins. This spin polarization

has a relatively large effect on the electronic properties with a clear differentiation between the 2 spins. For NO, an impurity band with a predominant weight of the PDOS of the molecule in the DOS is observed at the bottom of the CB for both spin (with slightly different energies). It can also be noticed a specific band just above the Fermi level for the spin down and one just below the Fermi level for the spin up. These bands, even if they have a significant dispersion, have no correspondence with the native bands of AGNR. For this reason, we do not expect any contribution of these bands to the transport. For NO₂ an isolated impurity band is observed for the down spin with a large weight of the PDOS of the Fe atom in the DOS. As mentioned earlier, this kind of band, with an energy within the gap of pristine AGNR, cannot have any implication in the

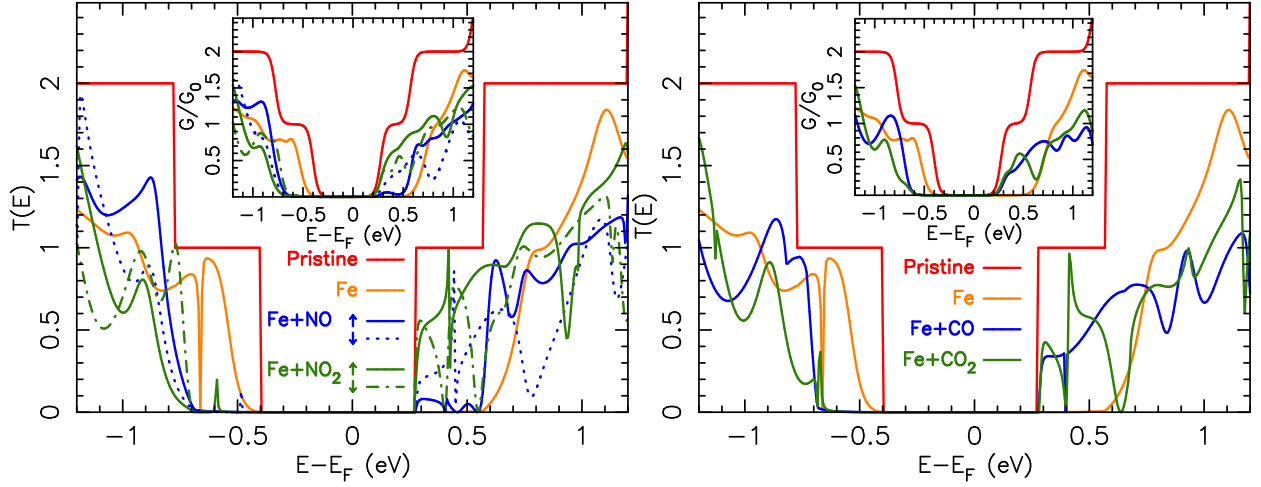


Figure 6: Transmission and electrical conductance (in inset) as function of the energy for pristine AGNR, Fe-AGNR and Fe-AGNR with CO, CO₂, NO and NO₂ molecules adsorbed on top of the Fe atom. For NO and NO₂ molecules, both spins are represented. The conductance is given as a fraction of the quantum of conductance G_0 and is computed at $T = 300$ K.

transport. Conversely to NO, no impurity band close to the bottom of the CB is observed. The signature of impurity band, with a large weight of the PDOS of NO₂ in the DOS, is found deeper in the VB (below 1 eV) and will thus have no role in the transport. It should be emphasized that the spin polarization observed for NO and NO₂ is induced by the adsorbed molecules. As we discussed in the next section the spin polarization occurs only in a region close to the defect. For this reason, these calculations which are performed under periodic conditions, cannot be directly transposed to interpret the transport properties with a single defect within the Landauer formalism. However, considering the large difference observed for the DOS between the 2 spins, we do expect a noticeable spin dependence on the scattering processes.

4. Transport properties

The transport properties of Fe-AGNR with adsorbed molecules (CO, CO₂, NO and NO₂) are given in Fig. 6. The results for pristine AGNR and Fe-AGNR are presented as benchmarks to quantify the influence of the adsorbed molecules on either the valence or the conduction band. The basic idea underlying this work is to propose strategies, based on the measurement of the electrical conductance, for the detection of gas molecules. For this reason the semiconducting devices considered here would need to be additionally p or n doped using either a co-dopant or by means of a

field effect set-up [52, 53] in order to tune the carrier concentration either of the valence or the conduction band.

The substitution of a carbon atom with an iron one is modifying significantly both the valence and the conduction band as pointed out in Ref. [34]. However, the influence of gas molecules as CO, NO or NO₂ adsorbed on it still needs to be addressed. When compared to the case of Fe-AGNR, the adsorption of the CO₂ molecule is modifying the transmission for both the valence and the conduction band. For the VB, the amplitude of the transmission of Fe-AGNR is significant when compared to pristine AGNR. However, with the CO₂ molecule, the transmission is fully suppressed. For the CB, the situation is reversed. Without the molecule the transmission is null, and with the molecule it becomes significant. This clearly proves that Fe-AGNR may play a crucial role for the detection of CO₂ molecules. **The influence of the CO molecule is very similar to the one observed with CO₂. The conductance is a little bit larger for the valence band, which could be a way to discriminate the 2 molecules.**

As already mentioned, NO and NO₂ molecules lead to a spin polarization and a large difference is observed on the transport properties between the 2 spins. For both molecules, a drastic reduction of the conduction is observed in the VB when compared to Fe-AGNR. At the bottom of the CB, the adsorption of both molecules tends to restore the conduction when compared to

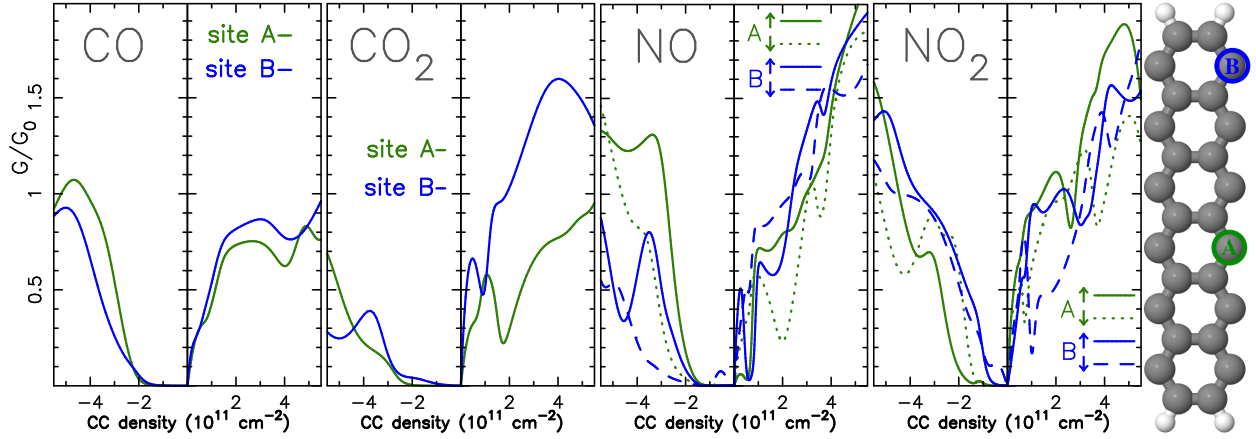


Figure 7: Electrical conductance (as a fraction of the quantum of conductance G_0) at $T = 300$ K as function of the carrier charge (CC) density for Fe-AGNR with CO, CO₂, NO and NO₂ molecules (both spins for NO and NO₂) adsorbed on top of the Fe atom for 2 different substitution sites (denoted A and B). The site A is the one considered previously and the site B is located at the edge of the AGNR. Negative CC density corresponds to hole doping and positive CC density to electron doping. The right figure depicts an AGNR strip the 2 substitution sites.

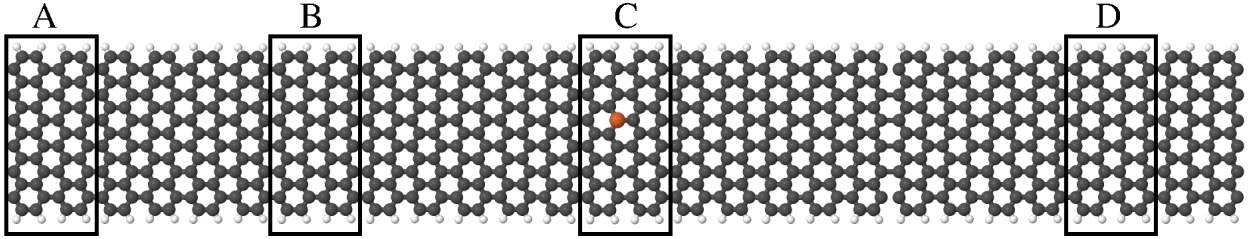


Figure 8: Molecular representation of the Fe-AGNR device considered to compute the LDOS presented in Fig. 9 and 10. The labels A,B,C and D refer to the sections of the ribbon on which the LDOS is computed.

Fe-AGNR knowing that NO₂ is leading to a larger conduction than NO. A detection of NO₂ gas molecules using this variation of the conductance at the bottom of the CB may be achievable. The differences between the two spins for NO₂ in the CB seem mainly related to the impurity bands (which have different energies for the 2 spins) which are leading to peaked reduction of the transmission. However, these variations are mostly blurred for the conductance at room temperature. For NO, the observed variations of the conductance at the bottom of the CB are smaller. However, a significant difference between the 2 spin is noticeable which could allow to detect the presence of NO molecules by measuring the difference between the conductance of the 2 spins.

In Fig.7, the electrical conductance is given as function the carrier charge (CC) density which allows a direct comparison with experimental results [54]. The CC density is obtained by integration of the DOS. In order to have an insight on the influence of the

substitution site, we have considered here 2 different sites for Fe substitution. The site A (corresponding to the site considered so far) is at the center of the AGNR and the site B is at the edge of it. Both sites are leading to the same stable conformation for the molecules. It should be note that the site B is more stable than the site A (the total energy difference between the site A and B is 350 meV). However, in the context of the common technique of focused electron beam irradiation [33] to obtain substitution Fe doping, the location of the original C vacancy, and thus of the Fe atom, is linked with the location of the electron beam irradiation and not with energetic considerations.

For CO the conductance is almost identical for both sites even at large CC density. For CO₂, a more significant influence of the site can be noticed for electron doping above $2 \cdot 10^{11} \text{ cm}^{-2}$. As already mentioned, the conductance for hole doping is significantly larger for CO than CO₂. For instance, with a CC density of $-4 \cdot 10^{11} \text{ cm}^{-2}$, the conductance for CO is about $1 \times G_0$

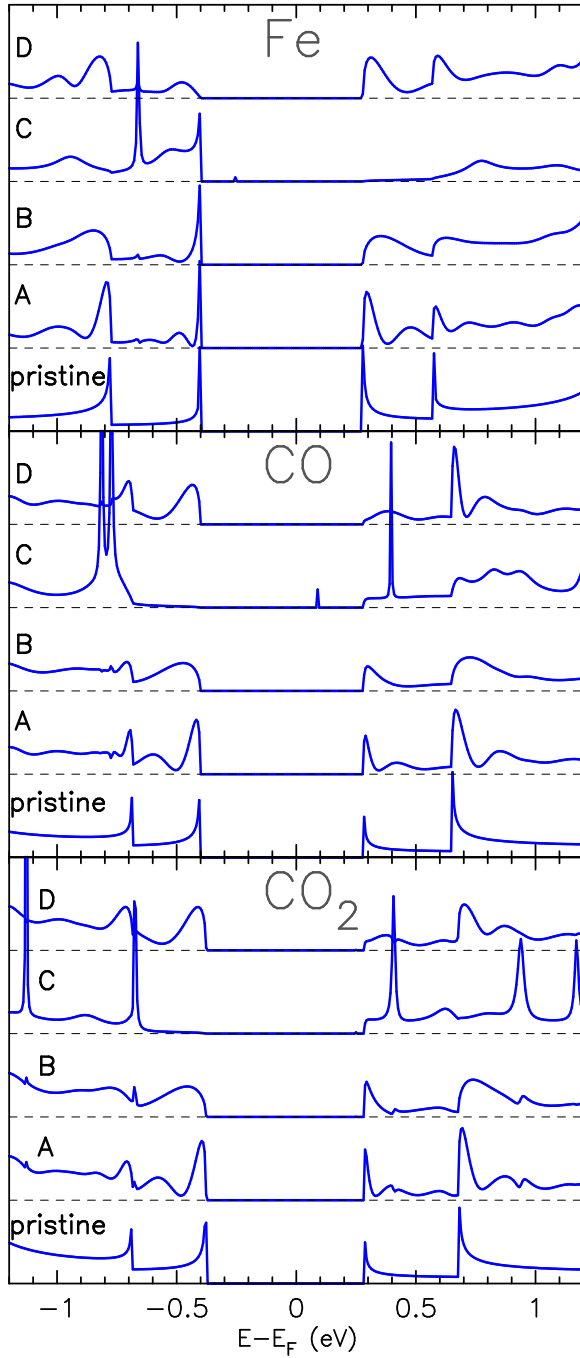


Figure 9: Local density of states along the device corresponding to Fe-AGNR and Fe-AGNR with CO or CO₂ molecule adsorbed on top of the Fe atom. For each case, is plotted the LDOS in one of the two leads (equivalent to pristine AGNR and denoted “pristine”) and in 4 different sections of the device denoted A, B, C and D. These sections are depicted in Fig. 8.

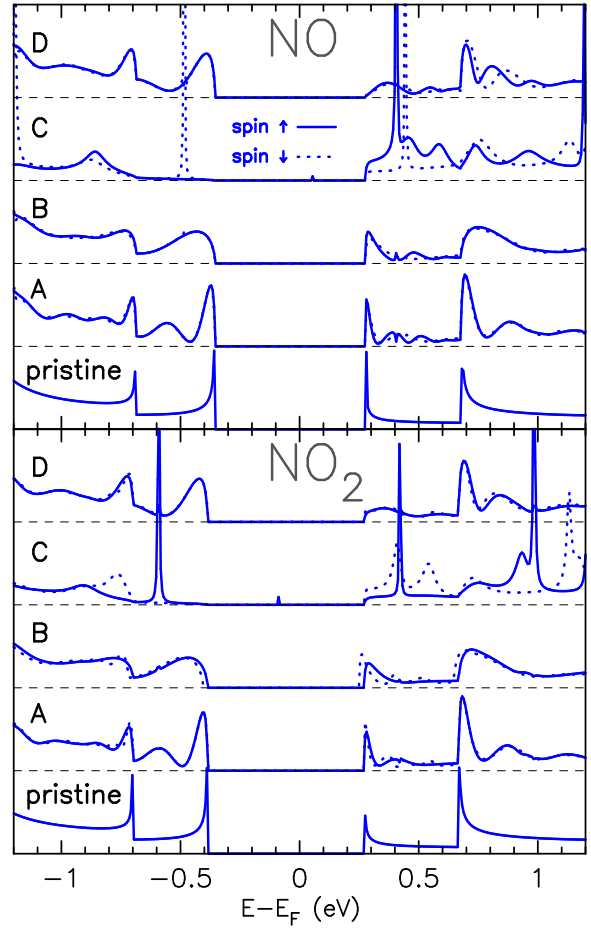


Figure 10: Local density of states along the device corresponding to Fe-AGNR with NO or NO₂ molecule adsorbed on top of it. For each case is plotted the LDOS in one of the two leads (equivalent to pristine AGNR and denoted “pristine”) and in 4 different sections of the device denoted A, B, C and D. These sections are depicted in Fig. 8. The LDOS associated to the spin up is represented with solid lines and to the spin down with dotted lines.

and about $0.3 \times G_0$ for CO₂. For NO, the variation of the conductance between the 2 spins mentioned previously is also observed for the site B. It is a little bit less pronounced for electron doping. For NO₂, the two sites are leading to very similar results. However, the sharp variations induced by impurity states are slightly shifted and are more pronounced for the site B.

To have a better understanding of the transport properties let us now investigate the local density of states (LDOS) of the devices. It can be computed by means of the Green’s function of the system [49, 55]. Its expres-

sion under equilibrium condition is:

$$\rho_i = -\frac{1}{\pi} \text{Im}[G_{ii}], \quad (3)$$

where the subscript i refers to one of the atomic orbitals and G_{ii} to one of the diagonal elements of the Green's function. For a system with a single defect such as Fe-AGNR with or without molecules, the LDOS far away from the defect (in the leads for instance) is equivalent to the DOS of pristine AGNR. It will differ and unveil the presence of the defect only in the vicinity of it. To investigate the modifications induced to the LDOS by the defect, we have considered 4 different strips of the ribbon located all along the device. These strips are presented in Fig. 8. The LDOS of each strip is obtained by summing ρ_i (see Eq. 3) over all the atomic orbitals of the atoms of the strip. The strip denoted A is 5.2 nm away from the defect, the strip B is 2.6 nm away, the strip C includes the defect and the strip D is 4.3 nm away in the opposite direction.

The LDOS for Fe-AGNR with and without CO or CO₂ are given in Fig 9. For comparison purposes, we also give the LDOS of one of the pristine lead (equivalent to pristine AGNR). The most noticeable influence of the defect with Fe-AGNR is on the CB. Fe is inducing a depletion of the LDOS on the strip C. This local gap is acting as a barrier for the transport, leading to the very poor transmission associated with this band observed in Fig. 6. Conversely, for the VB, the defect preserves the density in its neighborhood allowing a significant transport for this band. Concerning the influence of CO and CO₂ on the CB, **they both tend to restore the LDOS in their vicinity. This is the main reason why the conductance is restored at the bottom of the CB with these two molecules. By contrast, they are inducing a reduction of the LDOS at the top of the VB and consequently a reduction of the conductance.** It should be noted that the sharp peaks observed on the strip C for both CO and CO₂ correspond to impurity states. They induce some sharp variations of the transmission which are unnoticeable on the conductance at room temperature.

The LDOS with NO and NO₂ is given in Fig 10. It should be mentioned that the spin polarization is only noticeable close to the molecules. The LDOS of the 2 spins tend to be almost identical for the strips A and D which are the further away from the defect. It is on the strip C (which includes the defect) that the difference is the most significant. Both molecules tend to suppress the LDOS at the top of the VB. The only noticeable

LDOS on the strip C is due to impurity states. As already stated, this depletion of the LDOS is acting as a barrier leading to the null transmission observed with both NO and NO₂ in the VB. For the CB, the adsorption of the molecules restores the LDOS when compared to Fe-AGNR. However, the amplitude of the LDOS on the strip C is larger for NO than NO₂. For NO, this increase of the LDOS is related to impurity states as pointed out in Sec. 3 and is leading to a larger backscattering of the spin up.

5. Conclusion

In the present work, the possible strategies of toxic gas detection using **semiconducting** Fe doped armchair graphene nanoribbons are presented and the influence of the adsorption of gas molecules on the electronic and transport properties is discussed. We observe that Fe-AGNR is definitely a very good candidate for gas detection considering the high sensitivity of the electronic properties to the adsorption of molecules. **For CO₂ and CO, the measurement of the conductance at the bottom of the CB seems a promising method to detect these molecules. The measurement of the conductance at the top of the VB could be a way to discriminate the 2 molecules considering that CO is leading to a larger conductance.** NO and NO₂ molecules lead to a spin polarization of the system which is opening new perspectives to propose strategies for the detection of these molecules. For NO, we do observe a noticeable difference between the conductance of the 2 spins at the bottom of the CB. This difference could definitely be used to detect this kind of molecules using spin transport. On the other hand, with NO₂ a simple measurement of the variation of the conductance at the bottom of the CB seems the better option as the difference between the two spins is less obvious at room temperature.

References

- [1] A. K. Geim and K. S. Novoselov. *The rise of graphene*, pages 11–19. World Scientific, 2009.
- [2] N. K. Jaiswal and P. Srivastava. Fe-doped armchair graphene nanoribbons for spintronic/interconnect applications. *IEEE Transactions on Nanotechnology*, 12(5):685–691, 2013.
- [3] Gaurav Lalwani, Weiliang Xing, and Balaji Sitharaman. Enzymatic degradation of oxidized and reduced graphene nanoribbons by lignin peroxidase. *J. Mater. Chem. B*, 2:6354–6362, 2014.
- [4] Abhilash S. Singh, Suresh S. Shendage, and Jayashree M. Nagarkar. Electrochemical synthesis of copper nanoparticles on

- naflon-graphene nanoribbons and its application for the synthesis of diaryl ethers. *Tetrahedron Letters*, 55(35):4917 – 4922, 2014.
- [5] Ehsan Mahmoudi, Ali Hajian, Mosayeb Rezaei, Abbas Afkhami, Aziz Amine, and Hasan Bagheri. A novel platform based on graphene nanoribbons/protein capped Au-Cu bimetallic nanoclusters: Application to the sensitive electrochemical determination of bisphenol a. *Microchemical Journal*, 145:242 – 251, 2019.
- [6] K. S. Novoselov, A. K. Geim, S. V. Morozov, D. Jiang, Y. Zhang, S. V. Dubonos, I. V. Grigorieva, and A. A. Firsov. Electric field effect in atomically thin carbon films. *Science*, 306(5696):666–669, 2004.
- [7] Shuai Wang, Priscilla Kailian Ang, Ziqian Wang, Ai Ling Lena Tang, John T. L. Thong, and Kian Ping Loh. High mobility, printable, and solution-processed graphene electronics. *Nano Letters*, 10(1):92–98, 2010. PMID: 20025234.
- [8] K.I. Bolotin, K.J. Sikes, Z. Jiang, M. Klima, G. Fudenberg, J. Hone, P. Kim, and H.L. Stormer. Ultrahigh electron mobility in suspended graphene. *Solid State Communications*, 146(9):351 – 355, 2008.
- [9] Verónica Barone, Oded Hod, and Gustavo E. Scuseria. Electronic structure and stability of semiconducting graphene nanoribbons. *Nano Letters*, 6(12):2748–2754, 2006. PMID: 17163699.
- [10] F. Schedin, A. K. Geim, S. V. Morozov, E. W. Hill, P. Blake, M. I. Katsnelson, and K. S. Novoselov. Detection of individual gas molecules adsorbed on graphne. *Nature Materials*, 6:652–655, 2007.
- [11] O. Leenaerts, B. Partoens, and F. M. Peeters. Adsorption of H₂O, NH₃, CO, NO₂, and NO on graphene: A first-principles study. *Phys. Rev. B*, 77:125416, Mar 2008.
- [12] Mohammad Javad Kiani, M.T. Ahmadi, E. Akbari, H. Karimi, and F.K. Che Harun. Graphene nanoribbon based gas sensor. In *Advanced Computational Engineering and Experimenting II*, volume 553 of *Key Engineering Materials*, pages 7–11. Trans Tech Publications Ltd, 7 2013.
- [13] Kyeong Min Cho, Soo-Yeon Cho, Sanggyu Chong, Hyeong-Jun Koh, Dae Woo Kim, Jihan Kim, and Hee-Tae Jung. Edge-functionalized graphene nanoribbon chemical sensor: Comparison with carbon nanotube and graphene. *ACS Applied Materials & Interfaces*, 10(49):42905–42914, 2018.
- [14] Y. You, J. Deng, X. Tan, N. Gorjizadeh, M. Yoshimura, S. C. Smith, V. Sahajwalla, and R. K. Joshi. On the mechanism of gas adsorption for pristine, defective and functionalized graphene. *Phys. Chem. Chem. Phys.*, 19:6051–6056, 2017.
- [15] Muhammad Ali, Saba Khan, Falah Awwad, and Nacir Tit. High gas-sensing selectivity of bilaterally edge-doped graphene nanoribbons towards detecting NO₂, O₂ and SO₃ gas molecules: Ab-initio investigation. *Applied Surface Science*, 514:145866, 2020.
- [16] L. Brey and H. A. Fertig. Electronic states of graphene nanoribbons studied with the dirac equation. *Phys. Rev. B*, 73:235411, Jun 2006.
- [17] Young-Woo Son, Marvin L. Cohen, and Steven G. Louie. Energy gaps in graphene nanoribbons. *Phys. Rev. Lett.*, 97:216803, Nov 2006.
- [18] S. Fujii T. Enoki and K. Takai. Zigzag and armchair edges in graphene. *Carbon*, 0:3141–3145, August 2012.
- [19] S. Ihnatsenka, I. V. Zozoulenko, and G. Kirczenow. Band-gap engineering and ballistic transport in edge-corrugated graphene nanoribbons. *Phys. Rev. B*, 80:155415, Oct 2009.
- [20] Hengyi Xu, T. Heinzl, and I. V. Zozoulenko. Edge disorder and localization regimes in bilayer graphene nanoribbons. *Phys. Rev. B*, 80:045308, Jul 2009.
- [21] J. Ruseckas A. Orlof and I. V. Zozoulenko. Effect of zigzag and armchair edges on the electronic transport in single layer and bilayer graphene nanoribbons with defects. *Phys. Rev. B*, 88:125409, sept 2013.
- [22] Zongling Ding, Jun Jiang, Huaizhong Xing, Haibo Shu, Ruibin Dong, Xiaoshuang Chen, and Wei Lu. Transport properties of graphene nanoribbon-based molecular devices. *Journal of Computational Chemistry*, 32(4):737–741, 2011.
- [23] E. R. Mucciolo, A. H. Castro Neto, and C. H. Lewenkopf. Conductance quantization and transport gaps in disordered graphene nanoribbons. *Phys. Rev. B*, 79:075407, Feb 2009.
- [24] Florian Banhart, Jani Kotakoski, and Arkady V. Krashennnikov. Structural defects in graphene. *ACS Nano*, 5, Jan 2011.
- [25] M. Terrones H. Terrones, RuitaoLv and M. S. Dresselhaus. The role of the defects and doping in 2D graphene sheets and 1D nanoribbons. *Reports. Progress in Physics*, 75:062501, May 2012.
- [26] E J G Santos, A Ayuela, and D Sánchez-Portal. First-principles study of substitutional metal impurities in graphene: structural, electronic and magnetic properties. *New Journal of Physics*, 12(5):053012, may 2010.
- [27] S. Ihnatsenka and G. Kirczenow. Conductance quantization in strongly disordered graphene ribbons. *Phys. Rev. B*, 80:201407, Nov 2009.
- [28] Joonho Park, Heok Yang, K.-S. Park, and Eok-Kyun Lee. Effects of nonmagnetic impurities on the spin transport property of a graphene nanoribbon device. *The Journal of Chemical Physics*, 130(21):214103, 2009.
- [29] J. Liu, Z.H. Zhang, X.Q. Deng, Z.Q. Fan, and G.P. Tang. Electronic structures and transport properties of armchair graphene nanoribbons by ordered doping. *Organic Electronics*, 18:135–142, 2015.
- [30] L. Benchallal, S. Haffad, L. Lamiri, F. Boubenider, H. Zitoune, B. Kahouadji, and M. Samah. Theoretical study of Ag doping-induced vacancies defects in armchair graphene. *Physica B: Condensed Matter*, 538:150–153, 2018.
- [31] Ling Ma, Jian-Min Zhang, Ke-Wei Xu, and Vincent Ji. A first-principles study on gas sensing properties of graphene and Pd-doped graphene. *Applied Surface Science*, 343:121–127, 2015.
- [32] Miao Zhou, Yun-Hao Lu, Yong-Qing Cai, Chun Zhang, and Yuan-Ping Feng. Adsorption of gas molecules on transition metal embedded graphene: a search for high-performance graphene-based catalysts and gas sensors. *Nanotechnology*, 22(38):385502, aug 2011.
- [33] A. W. Robertson, B. Montanari, K. He, J. Kim, C.S. Allen, Y. A. Wu, J. Olivier, J. Neethling, N. Harrison, A. I. Kirkland, J. H. Warner. Dynamics of Single Fe Atoms in Graphene Vacancies. *Nano Letters*, 13(4):1468–1475, 2013.
- [34] G. R. Berdiyrov, H. Abdullah, M. Al Ezzi, G. V. Rakhmatullaeva, H. Bahloul, and N. Tit. CO₂ adsorption on Fe-doped graphene nanoribbons: First principles electronic transport calculations. *AIP Advances*, 6(12):125102, 2016.
- [35] Z. Gao, Y.Sun, M. Li, W. Yang and X. Ding. Adsorption sensitivity of Fe decorated different graphene supports toward toxic gas molecules (CO and NO). *Applied Surface Science*, 456:351–359, 2018.
- [36] F. W. N. Silva, A. L. M. T. Costa, Lei Liu and E B Barros. Intense conductivity suppression by edge defects in zigzag MoS₂ and WSe₂ nanoribbons: a density functional based tight-binding study. *Nanotechnology*, 27(44):445202, 2016.
- [37] F. W. N. Silva, E Cruz-Silva, M. Terrones, H. Terrones and E B Barros. Transport properties through hexagonal boron nitride clusters embedded in graphene nanoribbons. *Nanotechnology*, 27(18):185203, 2016.
- [38] L. Benchallal, S. Haffad, F. Boubenider, L. Lamiri, H. Zitoune, B. Kahouadji, and M. Samah. Ab initio study of iron adatom-

- vacancies in armchair graphene nanoribbons. *Solid State Communications*, 276:9 – 13, 2018.
- [39] José M. Soler, Emilio Artacho, Julian D. Gale, Alberto García, Javier Junquera, Pablo Ordejón, and Daniel Sánchez-Portal. The siesta method for ab initio order-N materials simulation. *J. Phys.: Condens. Matter*, 14:2745–2779, 2002.
- [40] J.P. Perdew, K. Burke, and M. Ernzerhof. Generalized gradient approximation made simple. *Physical Review Letters*, 77:3865–3868, 1996.
- [41] N. Troullier and José Luis Martins. Efficient pseudopotentials for plane-wave calculations. *Physical Review B*, 43:1993–2006, 1991.
- [42] Bing Huang, Zuanyi Li, Zhirong Liu, Gang Zhou, Shaogang Hao, Jian Wu, Bing-Lin Gu, and Wenhui Duan. Adsorption of gas molecules on graphene nanoribbons and its implication for nanoscale molecule sensor. *The Journal of Physical Chemistry C*, 112(35):13442–13446, 2008.
- [43] Diego Cortés-Arriagada, Nery Villegas-Escobar, Sebastián Miranda-Rojas, and Alejandro Toro-Labbé. Adsorption/desorption process of formaldehyde onto iron doped graphene: a theoretical exploration from density functional theory calculations. *Phys. Chem. Chem. Phys.*, 19:4179–4189, 2017.
- [44] J.K. Zak, E. Negro, I.A. Rutkowska, B. Dembinska, V. Di Noto, and P.J. Kulesza. Graphene-based nanostructures in electrocatalytic oxygen reduction. In Klaus Wandelt, editor, *Encyclopedia of Interfacial Chemistry*, pages 651 – 659. Elsevier, Oxford, 2018.
- [45] Shen-Lang Yan, Meng-Qiu Long, Xiao-Jiao Zhang, and Hui Xu. The effects of spin-filter and negative differential resistance on Fe-substituted zigzag graphene nanoribbons. *Physics Letters A*, 378(13):960 – 965, 2014.
- [46] S. GolafroozShahri, M.R. Roknabadi, N. Shahtahmasebi, and M. Behdani. Ab-initio investigation of spin-dependent transport properties in Fe-doped armchair graphyne nanoribbons. *Journal of Magnetism and Magnetic Materials*, 420:56 – 61, 2016.
- [47] Daniel S. Fisher and Patrick A. Lee. Relation between conductivity and transmission matrix. *Phys. Rev. B*, 23:6851–6854, Jun 1981.
- [48] Christophe Adessi, Stephan Roche, and X. Blase. Reduced backscattering in potassium-doped nanotubes: Ab initio and semiempirical simulations. *Physical Review B*, 73:125414, 2006.
- [49] Mads Brandbyge, José-Luis Mozos, Pablo Ordejón, Jeremy Taylor, and Kurt Stokbro. Density-functional method for nonequilibrium electron transport. *Physical Review B*, 65:165401, 2002.
- [50] Benchallal Lotfi; Haffad Slimane; Lamiri Lyes; Boubenider Fouad; Zitoune Hachemi; Kahouadji Badis; Samah Madani. Density functional theory study of gold doped armchair graphene nanoribbons with vacancies. *Journal of Computational and Theoretical Nanoscience*, 15:1484–1489, May 2018.
- [51] R. C. Longo, J. Carrete, and L. J. Gallego. Magnetism of substitutional Fe impurities in graphene nanoribbons. *The Journal of Chemical Physics*, 134(2):024704, 2011.
- [52] Xiaolin Li, Xinran Wang, Li Zhang, Sangwon Lee, and Hongjie Dai. Chemically derived, ultrasmooth graphene nanoribbon semiconductors. *Science*, 319(5867):1229–1232, 2008.
- [53] L. Jiao, L. Zhang, X. Wang, G. Diankov, and H. Dai. Narrow graphene nanoribbons from carbon nanotubes. *Nature*, 458:877–880, 2009.
- [54] S. Tanabe, Y. Sekine, H. Kageshima, M. Nagase, and H. Hibino. Carrier transport mechanism in graphene on SiC(0001). *Physical Review B*, 84:115458, 2011.
- [55] S. Datta. *Quantum transport: Atom to transistor*. Cambridge

University Press, Cambridge, United Kingdom, 2005.